Cellular/Molecular

Calmodulin Binds to the C Terminus of Sodium Channels $Na_v1.4$ and $Na_v1.6$ and Differentially Modulates Their Functional Properties

Raimund I. Herzog, Chuanju Liu, Stephen G. Waxman, and Theodore R. Cummins

Department of Neurology and Paralyzed Veterans of America/Eastern Paralyzed Veterans Association Neuroscience Research Center, Yale School of Medicine, New Haven, Connecticut 06510, and Rehabilitation Research Center, Veterans Affairs Connecticut Healthcare, West Haven, Connecticut 06516

Modulation of voltage-gated sodium channels (VGSC) can have a major impact on cell excitability. Analysis of calmodulin (CaM) binding to GST-fusion proteins containing the C-terminal domains of $Na_v1.1$–$Na_v1.9$ indicates that some of the tetrodotoxin-sensitive VGSC isoforms, including $Na_V1.4$ and $Na_V1.6$, are able to bind CaM in a calcium-independent manner. Here we demonstrate that association with CaM is important for functional expression of $Na_V1.4$ and $Na_V1.6$ VGSCs. Disrupting the interaction between CaM and the C terminus of $Na_V1.4$ and $Na_V1.6$ channels reduced current amplitude by 99 and 62%, respectively. Overexpression of CaM increased the current generated by $Na_v1.4$ and $Na_v1.6$ C-terminal mutant constructs that exhibited intermediate current densities and intermediate binding affinities for CaM, demonstrating that this effect on current density was directly dependent on the ability of the C terminus to bind CaM. In addition to the effects on current density, calmodulin also was able to modulate the inactivation kinetics of $Na_v1.6$, but not $Na_v1.4$, currents in a calcium-dependent manner. Our data demonstrate that CaM can regulate the properties of VGSCs via calcium-dependent and calcium-independent mechanisms and suggest that modulation of neuronal sodium channels may play a role in calcium-dependent neuronal plasticity.

Key words: **sodium channel; sodium current; current amplitude; calmodulin; calcium/calmodulin; fast inactivation**

Introduction

Voltage-gated sodium channels (VGSCs) are the main carriers of current underlying the fast upstroke of action potentials in excitable cells. Modulation of VGSCs can regulate the function of the brain (Catterall, 2000) and muscle (Weiss and Horn, 1986). The activity of many channel proteins is regulated by calmodulin (CaM) (Levitan, 1999; Saimi and Kung, 2002), a 16.7 kDa protein that is expressed in virtually all eukaryotic cells. CaM can induce changes in target proteins via its binding per se and in response to changes in calcium concentration (Chin and Means, 2000). For example, the activity of sodium channels in *Paramecium tetraurelia* is CaM-dependent (Ling et al., 1992; Saimi and Ling, 1995), and CaM plays a crucial role in the modulation of calcium channels (Lee et al., 1999; Peterson et al., 1999; Zuhlke et al., 1999).

Several lines of evidence suggest that VGSCs might be modulated by CaM in muscle and neurons. A large number of CaM binding proteins have an isoleucine–glutamine (IQ) CaM binding motif (Bahler and Rhoads, 2002). Rhoads and Friedberg (1997) identified IQ motifs in the C termini of $Na_V1.1$–1.3 and predicted that these VGSCs might bind CaM. Indeed, experiments that used a GST-fusion protein consisting of a 27-amino-acid fragment of the C terminus of $Na_V1.2$ showed that CaM binds directly to the $Na_v1.2$ IQ motif in a calcium-independent manner (Mori et al., 2000). Two recent studies suggest that CaM can affect the activity of $Na_V1.4$ (Deschenes et al., 2002) and $Na_V1.5$ (Tan et al., 2002) muscle VGSCs by binding to their IQ motifs.

IQ motifs have been identified in proteins that bind CaM permanently or transiently. Some proteins with IQ motifs bind CaM independently of calcium, whereas others selectively bind calcium/CaM or calcium-free CaM (Jurado et al., 1999; Bahler and Rhoads, 2002). The core of the IQ motif is often IQXXXRGXXXR, although the first residue is variable and can be ambiguous for isoleucine, leucine, or valine. The last residue reportedly can be either arginine or lysine, and the seventh residue is not well conserved. Thus a more generalized IQ motif might be [I,L,V]QXXXRXXXX[R,K] (Bahler and Rhoads, 2002). After aligning the C termini sequences of all known VGSC isoforms (see Fig. 1*A*), we observed that the key residues in the region of the C terminus sharing homology with a 23-residue-long IQ motif (Schultz et al., 2000) were conserved to varying degrees.

In this study we asked whether CaM binding to $Na_V1.6$, a neuronal VGSC (Burgess et al., 1995; Schaller et al., 1995; Smith et al., 1998), had the same functional consequences as CaM binding to the skeletal muscle VGSC, $Na_V1.4$ (Trimmer et al., 1989).

Received April 30, 2003; revised July 22, 2003; accepted July 29, 2003.

This work was supported in part by grants from the National Multiple Sclerosis Society and the Rehabilitation Research and Development Service and Medical Research Services, Department of Veterans Affairs, and by gifts from the Paralyzed Veterans of America and Eastern Paralyzed Veterans Association (EPVA). R.H. was an EPVA Spinal Cord Research Fellow. We thank Bart Tofness for providing us with excellent technical assistance.

Correspondence should be addressed to Dr. Theodore R. Cummins, Stark Neuroscience Research Institute, Indiana School of Medicine, 950 West Walnut, Indianapolis, IN 46202. E-mail: trcummin@iupui.edu.

C. Liu's present address: Department of Orthopaedic Surgery, New York University School of Medicine, New York, NY 10003.

 0270-6474/03/238261-10$15.00/0

Our novel data show that CaM regulates the current density of both $Na_V1.4$ and $Na_V1.6$. In addition, we show that CaM regulates the kinetic properties of $Na_V1.6$ currents in a calcium-dependent manner. This work presents functional evidence for participation of VGSCs in the intricate CaM signaling network that is present within neurons (Marrion and Tavalin, 1998; Dolmetsch et al., 2001) and muscles (Hamilton et al., 2000).

Materials and Methods

Molecular biology. cDNAs corresponding to the C termini of all known voltage-gated sodium channels (Goldin et al., 2000) were generated by PCR. Rat brain or dorsal root ganglion (DRG) cDNA served as a template for $Na_V1.1$, 1.2, 1.3, 1.4, 1.5, 1.8, and 1.9. $Na_V1.6$ was amplified from mouse cDNA (Smith et al., 1998) and $Na_V1.7$ from a human cDNA construct (Klugbauer et al., 1995). PCR products were subcloned into *Eco*RI/*Bam*HI sites of the pGEX3X vector (Amersham Biosciences, Piscataway, NJ) to generate glutathione *S*-transferase (GST) fusion constructs.

All mutations were inserted into the respective sodium channel cDNA constructs by using the Quick Change XL (Stratagene, La Jolla, CA) mutagenesis kit, following the instructions of the manufacturer. Mutagenic primers were designed to introduce the appropriate base pair changes into the rat $Na_V1.4$ and the mouse $Na_V1.6$ sequences. Initially, both channels were made tetrodotoxin (TTX)-resistant by changing a pore tyrosine residue to a serine (Y401S in $Na_V1.4$ and Y371S in $Na_V1.6$) (Cummins et al., 2001) to allow currents to be isolated after expression in neurons and human embryonic kidney 293 (HEK293) cells. These two TTX-resistant channel constructs served as templates for all further mutagenesis. The plasmid $Na_v1.4$-RBG4 (Ukomadu et al., 1992) was used for the $Na_v1.4$ constructs. C-terminal truncation mutants of $Na_V1.4$ were made by introducing a stop codon at amino acid position 1741 (DEL1) after the IQ motif and at position 1719 (DEL2) before the IQ motif. Primers were designed to change $Na_V1.4$ amino acid residues ^{1727}IQ^{1728} to AQ, EQ, IA, IE, AA, and EE.

Construction of a mammalian expression vector encoding neuronal rat $Na_v1.6$ channel. These studies used a cDNA construct that encodes the mouse $Na_V1.6$ open reading frame. The complete open reading frame of mouse $Na_V1.6$, generously provided by Dr. A. Goldin (Smith et al., 1998), was excised from a pLCT1 oocyte expression vector first by digestion with *Aat*II and then by blunting the ends with T4 DNA polymerase, followed by digestion with *Xho*I to release the $Na_v1.6$ insert. A mammalian expression vector pcDNA3.1 (Invitrogen, San Diego, CA), modified to render it a low-copy vector (Klugbauer et al., 1995), was digested with *Apa*I; the ends were blunted with T4 DNA polymerase and then digested with *Xho*I. In a subsequent ligation reaction the two DNA pieces were joined to form a 13 kb plasmid. Isolates that displayed the expected *Bam*HI digestion pattern were verified by sequencing the entire $Na_V1.6$ insert. A TTX-resistant phenotype of $Na_V1.6$ ($Na_V1.6r$) was produced by converting tyrosine 371 to serine (Y371S) as previously described for the $Na_v1.3$ channel (Cummins et al., 2001). This point mutation was introduced into the channel sequence with the Quick Change XL mutagenesis kit (Stratagene), with two mutagenic primers designed according to the manufacturer's instructions. The mutant construct subsequently was verified by sequencing the whole $Na_v1.6$ insert. A similar approach was used to mutate the $Na_V1.6$ residues ^{1900}LQ^{1901} to EQ, LE, and EE.

A CaM–EGFP (enhanced green fluorescent protein) fusion construct was generated by PCR. Forward and reverse primers containing an *Eco*RI and *Bam*HI restriction site, respectively, were used to amplify a wild-type CaM DNA fragment from a rat brain cDNA library, which then was subcloned into a previously *Eco*RI/*Bam*HI-digested pEGFP-N1 vector (Clontech, Palo Alto, CA). A dominant-negative calcium-insensitive CaM mutant was generated by mutating the first aspartates of each of the four calcium-binding EF hand motifs to alanines (Putkey et al., 1989; Peterson et al., 1999). All constructs were verified by sequencing.

Expression and purification of GST-fusion proteins. For expression of GST-fusion proteins the appropriate plasmids (pGEX–C terminus–$Na_V1.1$–$Na_V1.9$) were transformed into *Escherichia coli* DH5α (Stratagene). Fusion proteins were affinity purified on glutathione–Sepharose beads, as previously described (Liu et al., 1999).

GST pull-down assay. To examine the binding of CaM to the C termini of all of the sodium channels as well as the mutants of the $Na_V1.4$ C terminus, *in vitro*, we incubated equal amounts of glutathione–Sepharose beads loaded with purified GST fusion proteins with 2 μg of bovine CaM in binding buffer AM-100 (Voit et al., 1997) at 4°C overnight. After being washed with binding buffer AM-100 four times, the bound proteins were released by boiling for 5 min in SDS-loading buffer and separated on a 12% SDS-PAGE. Subsequent immunoblot visualization was performed with monoclonal anti-CaM antibodies (Zymed, San Francisco, CA).

Coimmunoprecipitation. A HEK293 cell line that stably expressed rat $Na_v1.4$ was grown in 100 mm dishes to 80% confluence. Sister cultures then were transfected with 30 μg of CaM–EGFP cDNA or EGFP cDNA, using 30 μl of Lipofectamine 2000 (Invitrogen) transfection agent. After 24 hr the cells in each dish were lysed in 500 μl of cell lysis buffer. Fractions of the supernatants were saved for loading on the gel, and the rest of the cell extracts was incubated with 5 μl of polyclonal anti-GFP antibody (Clontech). Protein A-agarose (Invitrogen) then was used to precipitate the protein complexes at 4°C overnight. After extensive washes the proteins were eluted in SDS loading buffer, and CaM was visualized by immunoblotting with a panspecific anti-sodium channel antibody (Upstate Biotechnology, Lake Placid, NY) used at a 1:1000 dilution.

Electrophysiology. Standard whole-cell patch-clamp techniques were used as previously described (Cummins et al., 1998). All cells were held at −120 mV for 5 min before the measurement of peak sodium current amplitude. The currents of the TTX-resistant constructs were recorded in the presence of 250 nM TTX to minimize contamination from endogenous HEK293 sodium currents. The pipette solution contained (in mM): 140 CsF, 1 EGTA, 10 NaCl, and 10 HEPES, pH 7.3. The bathing solution contained (in mM): 140 NaCl, 3 KCl, 1 $MgCl_2$, 1 $CaCl_2$, and 10 HEPES, pH 7.3. HEK293 cells were transfected by using the calcium-phosphate precipitation technique as previously described (Cummins et al., 1998).

Culture of DRG neurons. DRG neurons were cultured as described previously (Caffrey et al., 1992). Briefly, the L4 and L5 DRG ganglia were harvested from adult $Na_V1.8$ null mice (Akopian et al., 1999). The DRG were treated with collagenase A (1 mg/ml) for 25 min and then collagenase D (1 mg/ml) and papain (30 U/ml) for 25 min, dissociated in DMEM and Ham's F-12 medium supplemented with 10% fetal bovine serum, and plated on glass coverslips. $Na_v1.8$ null neurons were kept under standard tissue culture conditions for 5–7 d before biolistic transfections. We previously showed that $Na_v1.8$ null DRG neurons do not express fast- or slow-inactivating TTX-resistant sodium currents (Cummins et al., 1999, 2001). Some $Na_v1.8$ null DRG neurons do express persistent TTX-resistant sodium currents (Cummins et al., 1999), but these currents are typically <1 nA after several days in culture and run down quickly in whole-cell recording configuration; therefore, these persistent TTX-resistant currents are not significant under the culture and recording conditions used in the present study.

Biolistic transfection of $Na_v1.8$ null DRG neurons. The Helios Gene Gun System (Bio-Rad Laboratories, Hercules, CA) was used for biolistic transfection of neurons. $Na_v1.6r$ or $Na_v1.4r$ DNA (10 μg) was mixed with 5 μg of GFP DNA in 50 μM spermidine and coprecipitated onto 1.6 μm gold particles with $CaCl_2$. The DNA gold suspension was washed twice in 100% ethanol and resuspended in 0.05% polyvinylpyrrolidone in ethanol; it was used for coating the inner wall of 10 inches of Tefzel tubing (Bio-Rad Laboratories). The tubing was dried by using ultrapure nitrogen and was cut into ~20 cartridges for the Helios Gene Gun. This process resulted in a density of 1 mg of gold particles per shot and 0.75 μg of total DNA per cartridge.

Immediately before biolistic transfection, the culture medium was removed from the Petri dish. The gene gun was held ~2 cm above the cells, and a pressure of ~120 psi was used to discharge the gold particles. A 70 μm nylon mesh (Small PartsMiami Lakes, FL) was placed just in front of the Helios Gene Gun barrel liner to achieve a more uniform distribution of gold particles (Wellmann et al., 1999). Within 24 hr the cells usually

showed expression of GFP, indicating a successful biolistic transfection. Electrophysiological studies were conducted 18–48 hr after transfection, and most of the cells that expressed GFP also expressed fast-inactivating TTX-resistant sodium currents. Because these currents are not observed in untransfected $Na_v1.8$ null neurons or $Na_v1.8$ null neurons transfected with GFP alone, this confirmed that most of the cells that expressed GFP also had been cotransfected successfully with the $Na_v1.6$ TTX-resistant channel.

Statistical analysis. One-way ANOVAs were used to test for differences between the experimental groups. The difference between pairs of individual data sets was tested by Fisher's least significant difference (LSD) multiple comparison test, and p values < 0.05 were considered to be significant. Where appropriate, data were compared with Student's t test. Data are expressed as the mean ± SEM.

Results

Several members of the VGSC family are able to bind CaM directly

Many proteins, including voltage- and ligand-gated channels, are regulated by CaM (Levitan, 1999; Zhu et al., 2001). Some proteins bind to CaM in a constitutive manner, whereas others are able to do so if calcium ions are present in a sufficiently high concentration. To determine to which category the VGSCs belong, we examined CaM binding in the presence and the absence of Ca^{2+} ions. In analogy to the experiments conducted with calcium channels (Peterson et al., 1999), we generated cDNAs of GST-fusion proteins of the complete C terminus of all of the known members of the VGSC family (Goldin et al., 2000), $Na_V1.1$ through $Na_V1.9$. We used the whole C terminus rather than shorter peptide fragments because studies have shown that residues outside the immediate CaM binding region can have significant effects on binding affinity (Peersen et al., 1997). After expression and purification we incubated the GST-fusion proteins overnight with 2 μg of bovine CaM in the presence and absence of calcium ions. Because binding occurred under these *in vitro* conditions, we could exclude the possibility that any other factors might have mediated the observed interaction. Immunoblotting with an anti-CaM antibody revealed isoform-specific differences in CaM binding (Fig. 1*B*). Under both high and low calcium conditions the fusion proteins of $Na_V1.2$, $Na_V1.4$, and $Na_V1.6$ exhibited very strong binding to calmodulin, suggesting that, like $Na_v1.2$ (Mori et al., 2000), $Na_V1.4$ and $Na_V1.6$ also might be considered as high-affinity targets for CaM. The C termini of $Na_V1.1$ and $Na_V1.3$ showed weaker binding but also were able to bind CaM in the presence and absence of Ca^{2+} ions. The C terminus of $Na_v1.7$ exhibited weak binding to CaM only in the low calcium condition. The three TTX-resistant sodium channels ($Na_V1.5$, $Na_V1.8$, and $Na_V1.9$) did not show detectable binding of CaM to their C termini in our assay. This assay indicates that, whereas the TTX-sensitive VGSC isoforms (with the noted exception of $Na_v1.7$) bind CaM to their C termini in the presence and absence of Ca^{2+} ions, the TTX-resistant isoforms probably exhibit a much lower affinity for CaM.

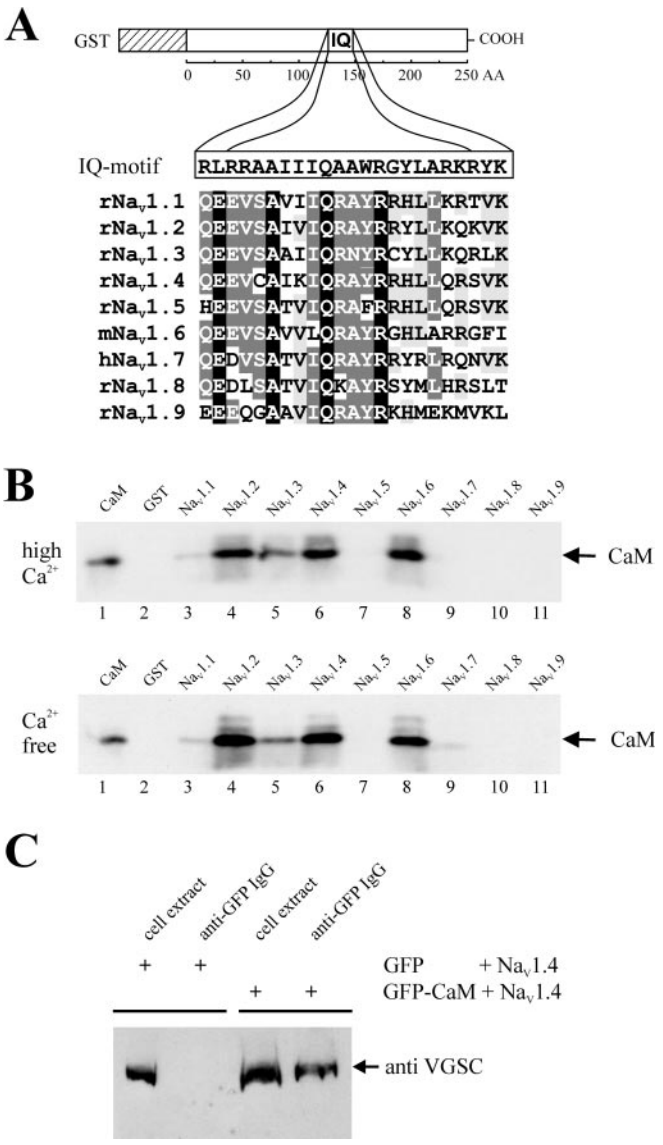

Figure 1. CaM binds to VGSC both *in vitro* and *in vivo*. *A*, Alignment of IQ motifs within VGSC C termini. Identical and highly conserved residues are shaded in black and gray, respectively. Shown is a schematic of a GST-fusion protein with the 250-amino-acid-long C terminus of a sodium channel, indicating the position of the highly conserved IQ motif (Schultz et al., 2000). *B*, GST pull-down assay shows that CaM binds to the C termini of VGSC with different affinity. Fusion proteins of the individual isoforms, as indicated above each lane, were tested for their *in vitro* capability to pull down CaM in the presence (5 mM $CaCl_2$; top row) and absence (2 mM EDTA; bottom row) of Ca^{2+}. Immunoblotting was performed with a monoclonal anti-CaM antibody. *C*, CaM associates with full-length $Na_v1.4$ in transfected HEK293 cells *in vivo*. Cell extracts from cells stably expressing rat $Na_v1.4$ that had been transfected either with EGFP cDNA (lanes 1, 2) or with CaM–EGFP cDNA (lanes 3, 4) were immunoblotted with an anti-CaM antibody. The immunoprecipitated proteins were visualized with a panspecific anti-VGSC antibody and show that CaM is required for a pull down of the $Na_V1.4$ channel.

CaM binds to $Na_V1.4$ *in vivo*

CaM binding to VGSCs has not been shown to occur in mammalian cells yet, raising the possibility that CaM may not bind to full-length channels. To address this issue, we performed a coimmunoprecipitation with the skeletal muscle sodium channel $Na_V1.4$, which showed high-affinity binding to CaM in the GST pull-down assay and has been well characterized (Ukomadu et al., 1992). We transfected a HEK293 cell line that stably expressed the rat $Na_V1.4$ channel with a plasmid encoding a CaM–EGFP fusion protein. It has been shown previously that EGFP does not interfere with normal CaM–target interactions (Erickson et al., 2001). A pull-down assay for the sodium channel protein complex, using a polyclonal anti-GFP antibody and a panspecific anti-sodium channel antibody for visualization, showed that CaM–EGFP was part of the sodium channel complex (Fig. 1*C*). This demonstrates that CaM truly can bind to the full-length $Na_V1.4$ protein in an *in vivo* environment. Electrophysiological examination of the currents produced by $Na_V1.4$ in this experiment revealed no change of any of its properties in comparison to the sister cultures expressing $Na_V1.4$ alone (data not shown).

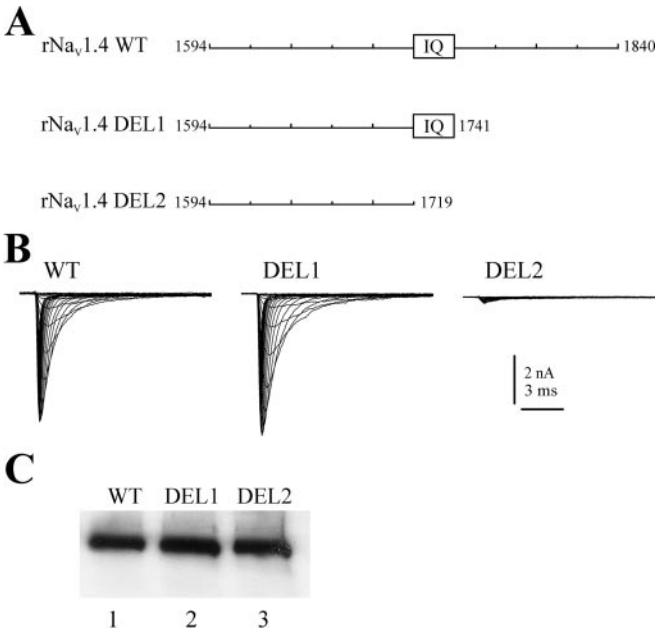

Figure 2. The IQ motif is required for VGSC currents. *A*, Schematic of C-terminal deletion constructs: wild-type rat $Na_V1.4$ (WT), C-terminal deletion mutant (DEL1) in which a stop codon has been inserted immediately after the IQ motif, and second deletion mutant (DEL2) in which the 23-residue-long IQ motif was removed also. *B*, The corresponding current recordings from HEK293 cells transfected with these three constructs are shown. Whereas the peak current amplitude of DEL1 (5.7 ± 0.9 nA; $n = 13$) is similar to that of wild-type Na_V 1.4 (4.9 ± 0.6 nA; $n = 45$), DEL2 exhibits little or no current (0.32 ± 0.04 nA; $n = 18$). *C*, Protein expression levels of deletion constructs. A Western blot of wild-type $Na_V1.4$, DEL1, and DEL2 in transiently transfected HEK293 cells with anti-VGSC panspecific antibody shows equal amounts of protein in each lane.

However, this cannot be interpreted as evidence that CaM does not alter the functional properties of $Na_v1.4$ channels. The data in Figure 1*B* suggest that $Na_v1.4$, like $Na_v1.2$, binds CaM with a high affinity. Because CaM is thought to be expressed in all eukaryotic cells, it is possible that the endogenous levels of CaM in HEK293 cells are sufficient to saturate $Na_v1.4$ channels; therefore, the expression of additional CaM has no further effect.

CaM directly modulates $Na_V1.4$ function

To investigate further the functional implications of the CaM–VGSC complex, we constructed two different C-terminal deletion mutants (Fig. 2*A*) and compared their sodium currents with those produced by the full-length $Na_V1.4$. In construct DEL1 we deleted the amino acids from the end of the C-terminal up to, but not including, the IQ motif. In construct DEL2 we deleted an additional 23 amino acids in the C terminus that comprise the IQ motif. Channel constructs were transiently expressed in HEK293 cells to determine whether the C-terminal region containing the IQ motif was functionally relevant. All of our electrophysiological measurements were conducted by using $Na_V1.4$ channels mutated to be TTX-resistant by changing the tyrosine at position 401 to serine (Y401S) and by recording in the presence of TTX to help differentiate our recombinant channel currents from the endogenous TTX-sensitive currents that are often present at low, but detectable, levels in HEK293 cells (Cummins et al., 1993). In this and subsequent experiments the term "wild-type $Na_v1.4$" will be used to refer to the TTX-resistant variant $Na_v1.4$-Y401S.

The currents produced by construct DEL1 (Fig. 2*B*) had activation and inactivation kinetics and peak amplitudes ($n = 15$) that were identical to those of the wild-type $Na_v1.4$ channel ($n = 44$), indicating that the distal portion of the C terminus is not vital for normal channel function in HEK293 cells. In contrast, the DEL2 construct produced little or no sodium current ($n = 18$) when tested with the same voltage-clamp protocol as the wild-type channel and construct DEL1, showing that the region containing the IQ motif is critical for the generation of inward current by $Na_V1.4$ (Fig. 2*B*). To determine whether the DEL2 construct produced protein levels comparable to wild-type $Na_V1.4$ and DEL1, we performed a Western blot with protein extracted from cells that were transfected, with the same amounts of DNA for all three constructs (Fig. 2*C*). Similar amounts of protein were produced by all three constructs, demonstrating that, although the IQ motif is necessary for $Na_V1.4$ current, it is not required for protein expression.

Prompted by this drastic effect of the DEL2 deletion on $Na_V1.4$ current density, we wanted to refine further our analysis of the importance of the IQ motif. Mutations that change the hydrophobicity and charge of the core residues isoleucine and glutamine of the CaM binding motif have been used previously to study the interaction of CaM with its targets (Peterson et al., 1999; Zuhlke et al., 2000; Deschenes et al., 2002). We designed $Na_v1.4$ constructs in which the corresponding amino acids were mutated to either alanines or glutamic acids and tested their electrophysiological properties. The isoleucine and the glutamine of the IQ motif (Fig. 1*A*) first were changed individually to either an alanine or a glutamic acid; then both residues were mutated together (Fig. 3*A*). Changing the isoleucine at position 1727 to the similar alanine (referred to as AQ) induced no significant changes in current properties when compared with the wild-type (IQ) channel. However, introducing a charged glutamic acid (EQ) at position 1727 reduced the peak sodium current by >90% (Fig. 3*D*). The remaining current is similar in amplitude to the endogenous TTX-resistant sodium current often observed in untransfected HEK293 cells (Cummins et al., 1999). In contrast, altering the second residue, glutamine 1728, to either alanine (IA) or glutamic acid (IE) reduced sodium currents by ~50% (Fig. 3*B*). Interestingly, neither the voltage dependence of activation and steady-state inactivation nor any of the time constants that were measured were different for the IE or for any other mutant that we compared with wild-type $Na_V1.4$ (IQ) (Fig. 3*C*). The double mutations, I1727A/Q1728A (AA) and I1727E/Q1728E (EE), reduced sodium currents to background levels (Fig. 3*B*,*D*), similar to the current reduction observed with construct DEL2 (Fig. 2*B*). This shows that the current reduction is not attributable to the addition of negative charges into the C terminus alone and suggests that it is attributable to disruption of the IQ motif.

To determine whether the observed amplitude changes were correlated with altered binding of CaM to the channel, we introduced the glutamic acid mutations EQ, IE, and EE into the GST-fusion protein of the $Na_V1.4$ C terminus and tested their ability to bind CaM (Fig. 3*E*). Changing IQ to IE reduced binding, and changing IQ to EQ or EE seemed to prevent binding of CaM to the C terminus completely. This correspondence between CaM binding of the different IQ mutants and peak current amplitudes provides evidence for a direct link between CaM binding and the regulation of current amplitude and suggests that the current reduction was not attributable to CaM-independent interactions.

If the hypothesis that the reduced current levels observed with the IE and IA mutant channels were the result of a lower affinity of CaM for the C terminus of these channels is correct, then increasing the intracellular CaM concentration should increase the current produced by the IE and IA mutant $Na_v1.4$ channels. In contrast, increasing CaM concentration would not be pre-

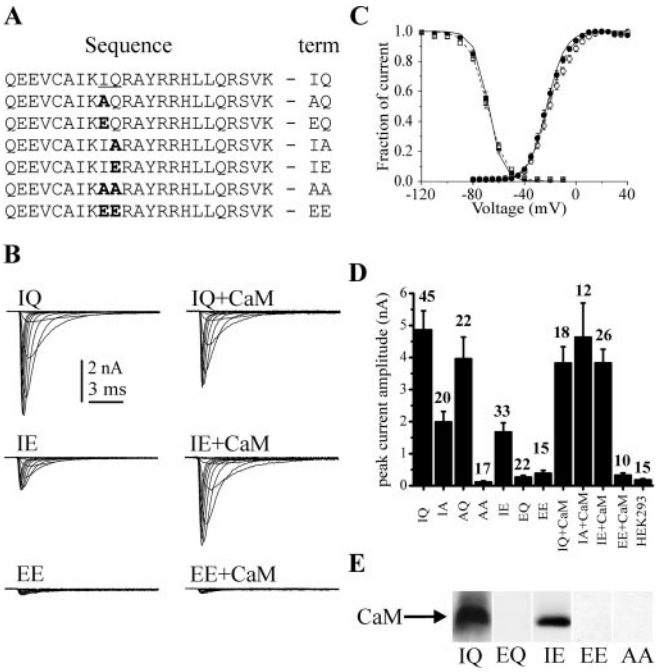

Figure 3. CaM binding is required for VGSC function. *A*, The portion of the C-terminal containing the CaM binding IQ motif is shown for wild-type $Na_v1.4$ (IQ) and the alanine and glutamic acid substitution mutants (boldface letters). *B*, Representative families of voltage-clamp recordings from HEK293 cells expressing wild-type $Na_v1.4$ (IQ), IE, and EE constructs are shown in the left column. The IE mutation caused a 60% reduction in peak current amplitude (2.0 ± 0.3 nA; $n = 20$) as compared with wild-type channels (4.9 ± 0.6 nA; $n = 45$), and the EE mutation nearly eliminated currents (0.39 ± 0.09 nA; $n = 15$). Increasing the available intracellular CaM by coexpressing the channel constructs with CaM–EGFP (right column) increased the peak current amplitude of the IE construct (3.8 ± 0.4 nA; $n = 26$) but had no effect on IQ amplitude (3.8 ± 0.5 nA; $n = 18$) or on the amplitude of the EE double mutant (0.33 ± 0.07 nA; $n = 10$). Cells were held at −120 mV, and currents were elicited by 40 msec test pulses to potentials ranging from −80 to −40 mV. *C*, Mutation of IQ does not induce changes in voltage dependence of activation or steady-state inactivation. Comparison of a mutant that produced intermediate current amplitudes (IE; open symbols) with wild-type $Na_v1.4$ (filled symbols) revealed an identical voltage dependence of activation and inactivation. *D*, Shown are peak current amplitudes of $Na_v1.4$ constructs in which the core residues of the CaM binding IQ motif were replaced. The number of cells recorded from for each group is indicated above the bars. ANOVA plus pairwise comparisons (Fisher's LSD multiple comparison test) revealed that the AA, EQ, and EE current amplitudes were significantly lower than wild-type (IQ) current amplitudes, but not different from the amplitude of endogenous TTX-resistant currents in untransfected HEK293 cells (0.18 ± 0.03 nA). The AQ current amplitudes were not significantly different from wild-type (IQ) current amplitudes. Two mutants, IA and IE, produced intermediate current amplitudes that were significantly different (Fisher's LSD multiple comparison test, $p > 0.05$) from both wild-type $Na_v1.4$ (IQ) and endogenous HEK293 current amplitudes. Overexpression of CaM significantly increased the current in cells expressing intermediate mutants (IA+Cam, and IE+CaM), but not wild-type (IQ+CaM) or EE (EE+CaM) channels. *E*, Changing I and Q alone affects CaM binding in a GST pull-down assay. The same mutations as above were introduced into the fusion proteins of the C terminus of $Na_v1.4$. The EQ, EE, and AA mutations drastically reduced CaM binding, but the IE mutation showed an intermediate affinity.

dicted to increase the current produced by the EE mutant, because this double mutation appeared to eliminate CaM binding to the C terminus of $Na_v1.4$. Therefore, we tested whether overexpression of CaM was able to rescue the loss of current observed with the IQ mutants. We coexpressed the CaM–EGFP construct with wild-type $Na_V1.4$, the IE and IA mutant constructs that produced intermediate current amplitudes, and the EE construct, which produced little or no current (Fig. 3*B*). Higher intracellular CaM concentrations had no significant influence on current amplitude (Fig. 3*D*) or voltage dependence of the wild-type channel (data not shown). Although we did not observe an increase in current with the EE mutant, which eliminated CaM binding in the GST-fusion protein assay, overexpression of CaM boosted the current of the intermediate IE and IA constructs to wild-type current levels (Fig. 3*B*,*D*). These data confirm that CaM can regulate $Na_V1.4$ sodium current density directly by binding to the C terminus.

CaM also modulates $Na_V1.6$ current amplitude

We next asked whether neuronal VGSC isoforms might be regulated by CaM in the same manner as $Na_v1.4$. The initial GST pull-down assay indicated that $Na_V1.6$, an isoform that is very abundant in brain (Burgess et al., 1995; Tzoumaka et al., 2000), binds CaM with an affinity comparable to that of $Na_V1.4$ and $Na_v1.2$. The IQ motif of $Na_V1.6$ is slightly different from that of the other VGSCs (Fig. 1*A*) in that $Na_V1.6$ has a leucine instead of an isoleucine at the position corresponding to I1727 of $Na_V1.4$. However, this residue of the IQ motif has been shown to be variable in conventional myosins, and isoleucine, leucine, or valine generally is considered equivalent at this position (Bahler and Rhoads, 2002). In addition, the I1727L mutation had no effect on the functional properties of $Na_v1.4$ (data not shown). To test the functional consequences of CaM binding to the IQ motif of $Na_V1.6$, we mutated two of the core residues of the IQ motif in $Na_V1.6$, residues L1900 and Q1901, to glutamates. We compared the properties of wild-type $Na_V1.6$ channels (LQ) with $Na_V1.6$-Q1901E (LE) and $Na_V1.6$-L1900E-Q1901E (EE) mutant channels. Because $Na_V1.6$ channels express poorly in HEK cells (0.31 ± 0.05 nA; $n = 30$), we used a TTX-resistant variant of $Na_V1.6$ ($Na_V1.6$-Y371S) expressed in DRG neurons from $Na_V1.8$ null mice (Akopian et al., 1999). After 5 d in culture these neurons lack TTX-resistant currents and therefore provide a very suitable expression system for expression of sodium channels that have been mutated to be TTX-resistant (Cummins et al., 2001).

At 24 hr after biolistic transfection large (peak amplitude, 40.8 ± 4.0 nA; $n = 31$) $Na_V1.6$ sodium currents (Fig. 4*A*) were recorded in the presence of 250 nM TTX. The currents produced by the LE construct were 74% smaller than wild-type (LQ) currents (Fig. 4*B*). In contrast to the effect of the IQ mutations on $Na_V1.4$, the $Na_v1.6$ construct with the EE double mutation reduced $Na_V1.6$ current amplitudes down to only ~37% of control (Fig. 4*A*,*B*). ANOVA plus pairwise comparisons (Fisher's LSD multiple comparison test) revealed that the mutant current amplitudes were significantly smaller than wild-type current amplitude but that the difference between the current amplitudes produced by LE and EE mutants was not significant. To determine whether the difference in the effect of the EE double mutation on $Na_V1.4$ and $Na_V1.6$ current amplitude was the result of the different expression backgrounds (HEK293 cells vs DRG neurons), we expressed $Na_V1.4$ and $Na_V1.4$-EE channels in $Na_V1.8$ null DRG neurons. Because we were using TTX-resistant constructs, we again were able to isolate the transfected currents by using 250 nM TTX. Although large TTX-resistant sodium currents were recorded from neurons transfected with $Na_V1.4$ channels, virtually no current was observed in neurons transfected with $Na_V1.4$-EE channels (Fig. 4*B*). It is not clear what accounts for the difference in the effect of the EE double mutation on $Na_V1.4$ and $Na_V1.6$ current amplitude, but it could reflect additional binding sites for CaM on $Na_V1.6$ channels, as has been reported for some L-type calcium channels (Pitt et al., 2001).

In analogy to the study of $Na_V1.4$, we wanted to determine whether the modulation of $Na_v1.6$ current amplitude by the IQ motif mutations depended on the reduced binding of CaM to the

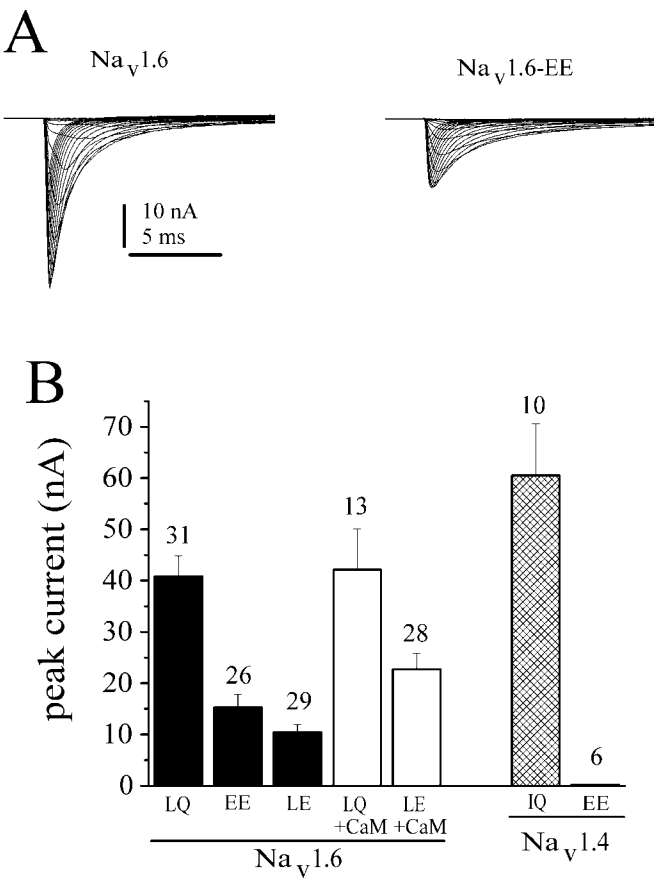

Figure 4. The IQ motif of $Na_v1.6$ channels is an important determinant of current amplitude. *A*, Representative families of voltage-clamp recordings from $Na_v1.8$ null DRG neurons TTX-resistant $Na_V1.6$ (left) and $Na_V1.6$-EE (right) channels are shown. Cells were held at −120 mV, and currents were elicited by 40 msec test pulses to potentials ranging from −80 to −40 mV in 5 mV increments. *B*, Shown are peak current amplitudes of $Na_v1.6$ and $Na_v1.4$ constructs in which the core residues of the CaM binding IQ motif were replaced. The number of neurons recorded from for each group is indicated above the bars. ANOVA plus pairwise comparisons (Fisher's LSD multiple comparison test) revealed that the $Na_v1.6$-LE and $Na_v1.6$-EE mutant channels produced lower current amplitudes than wild-type (LQ) $Na_v1.6$ channels (black bars) and that overexpression of CaM increased the current amplitude produced by $Na_v1.6$-LE mutant channels, but not wild-type channels (open bars). The EE double mutant reduced the amplitude of currents produced by $Na_v1.4$ channels expressed in DRG neurons by >99% (shaded bars).

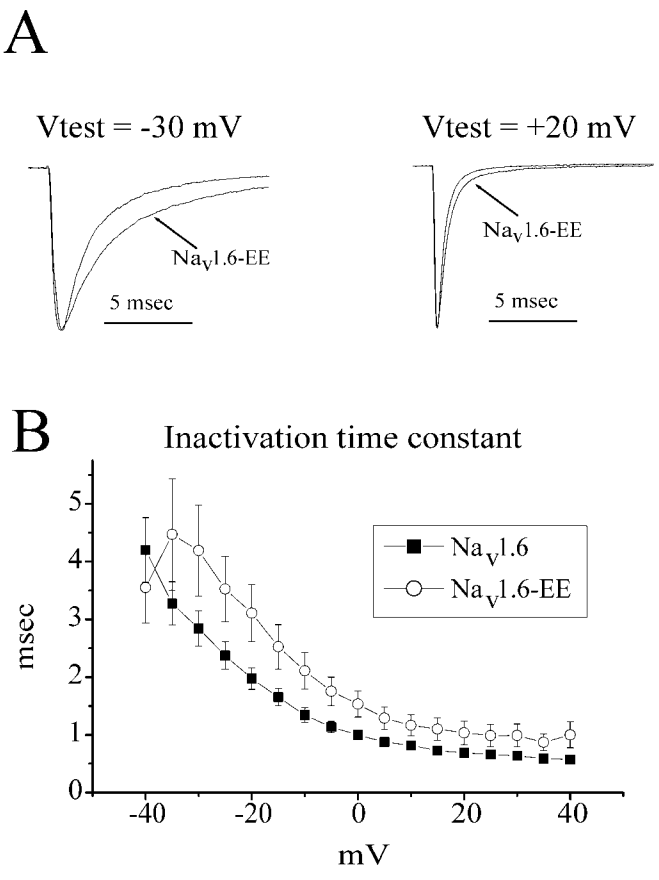

Figure 5. The EE mutation in the IQ motif alters the inactivation kinetics of $Na_v1.6$ channels. *A*, Comparison of representative traces from $Na_v1.8$ null DRG neurons transfected with wild-type and EE mutant $Na_v1.6$ channels. Currents were elicited with test pulses to −30 mV (left) and +20 mV (right). The EE mutant channels exhibited slower inactivation. *B*, Inactivation kinetics as a function of voltage. The macroscopic decay time constant is greater for $Na_v1.6$ EE currents (open circles; $n = 8$) than for $Na_v1.6$ wild-type currents (filled squares; $n = 16$) at all voltages ranging from −25 to +40 mV (Student's t test, $p < 0.05$). Time constants were estimated from single exponential fits to the decay phase of currents elicited by 40 msec step depolarizations to the indicated potential.

channel. Therefore, we tested whether overexpression of CaM could rescue the reduced current of the LE construct. The LE current amplitude was increased by 118% (Student's t test, $p < 0.001$) when more CaM was available to the channel. As with $Na_V1.4$, this change in current density was not associated with changes in the voltage dependence of activation or inactivation.

Time course of inactivation varies between wild-type $Na_V1.6$ (LQ) and EE mutant currents

Although the activation time constant τ_m did not differ between the LQ and EE $Na_V1.6$ channel constructs, there was a significant difference (Student's t test, $p < 0.05$) in the inactivation time constant τ_h between LQ and the EE constructs (Fig. 5). The EE double mutation slowed $Na_V1.6$ inactivation by 48% at −30 mV and 51% at +20 mV. The rate of fast inactivation was slower for the EE mutant channels at all voltages from −30 to +40 mV. Because shifts in the voltage dependence of channel gating can contribute to changes in inactivation kinetics, we compared the voltage dependence of activation and steady-state inactivation for $Na_V1.6$ LQ and EE constructs. The midpoints for activation (determined with a Boltzmann function) were not significantly different for LQ (−25.4 ± 1.0 mV; $n = 7$) and EE (−22.9 ± 2.4 mV; $n = 8$) $Na_v1.6$ currents. The midpoints for steady-state inactivation were also similar for LQ (−64.3 ± 2.1 mV; $n = 10$) and EE (−65.5 ± 2.0 mV; $n = 9$) $Na_v1.6$ currents. Thus shifts in the voltage dependence of channel gating do not seem to contribute to the differences in inactivation kinetics.

Calcium/calmodulin switches $Na_V1.6$ from a fast into a slow mode

In the GST pull-down assay we showed that CaM binds to $Na_V1.6$ in the presence and absence of calcium ions. However, CaM is considered the prototype of a family of intracellular calcium sensor proteins that confer calcium sensitivity to their targets (Chin and Means, 2000; Burgoyne and Weiss, 2001). Because reducing the binding of CaM to $Na_V1.6$ changes its inactivation kinetics, we asked whether this reflects a physiologically relevant CaM-dependent mechanism that also could be regulated by changes in intracellular calcium concentration. All of the experiments described above were conducted with low intracellular calcium in which the pipette solution contained 1.1 mM EGTA and no added calcium. Similar results were obtained with 20 mM BAPTA and no added calcium in the pipette. To examine $Na_V1.6$ current

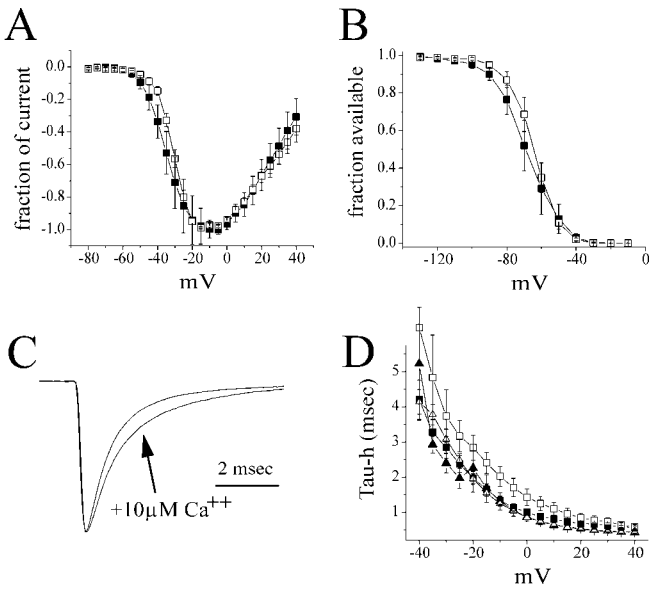

Figure 6. Calcium/CaM modulates $Na_v1.6$ inactivation kinetics, but not voltage-dependent properties. *A*, Normalized peak current–voltage relationship for TTX-resistant $Na_v1.6$ channels recorded with low (filled squares; $n = 5$) and high (open squares; $n = 6$) intracellular calcium. The currents were elicited by 40 msec test pulses to various potentials from −80 to −40 mV. Cells were held at −120 mV. *B*, Comparison of TTX-resistant $Na_v1.6$ steady-state inactivation recorded with low (filled squares; $n = 5$) and high (open squares; $n = 6$) intracellular calcium. Steady-state inactivation was estimated by measuring the peak current amplitude elicited by 20 msec test pulses to −10 mV after 500 msec prepulses to potentials over the range of −130 to −10 mV. Current is plotted as a fraction of the maximum peak current. *C*, Representative currents from whole-cell recordings of $Na_v1.8$ null DRG neurons expressing TTX-resistant $Na_v1.6$ channels in high or low intracellular calcium. Currents were elicited by a step depolarization to −10 mV from a holding potential of −120 mV and were scaled for comparison. The current recorded in high calcium displays slower kinetics. *D*, Inactivation kinetics as a function of voltage for $Na_v1.6$ currents. The macroscopic decay time constant is greater for TTX-resistant $Na_v1.6$ currents recorded with high intracellular calcium (open squares; $n = 6$) than with low intracellular calcium (filled squares; $n = 16$) or for TTX-resistant $Na_v1.6$ currents coexpressed with calcium-deficient CaM_{1234} with either high (open triangles; $n = 5$) or low (filled triangles; $n = 5$) intracellular calcium. Time constants were estimated from single exponential fits to the decay phase of currents elicited by 40 msec step depolarizations to the indicated potential. All recordings were made in the presence of 250 nM TTX from $Na_v1.8$ null DRG neurons transfected with TTX-resistant $Na_v1.6$ channels. Significant differences were determined using Student's *t* test with the significance value set at $p < 0.05$.

properties at a high $[Ca^{2+}]_i$, we added 1.1 mM calcium to the pipette solution that contained 1.1 mM EGTA, which raised the free calcium level to ~10 μM. We also examined the effect of a CaM mutant in which the aspartates in the first position of the four calcium-binding EF hand motifs had been replaced by an alanine to render it calcium-insensitive. This mutant usually is referred to as a dominant-negative form of CaM and is abbreviated as CaM_{1234} (Peterson et al., 1999; Pitt et al., 2001).

We first examined the effect of coexpression of wild-type CaM with $Na_V1.6$ on $Na_V1.6$ current characteristics. Coexpression of wild-type CaM with $Na_V1.6$ did not alter the properties of currents recorded with low $[Ca^{2+}]_i$. Raising $[Ca^{2+}]_i$ in the presence of overexpressed CaM did not alter the voltage dependence of activation (Fig. 6*A*) or steady-state inactivation (Fig. 6*B*). However, with high $[Ca^{2+}]_i$ the currents recorded from cells transfected with $Na_V1.6$ and CaM exhibited slower time constants of inactivation (Fig. 6*C*,*D*). On the other hand, when $Na_V1.6$ channels were coexpressed with CaM_{1234}, the inactivation kinetics were fast in the presence of both high and low $[Ca^{2+}]_i$ (Fig. 6*D*). Thus high $[Ca^{2+}]_i$ with wild-type CaM, but not with the calcium-insensitive CaM_{1234}, had the same effect on the rate of inactivation as did the EE double mutation. This indicates that calcium-free CaM can enhance the rate of $Na_v1.6$ inactivation.

For comparison, we also tested the calcium sensitivity of $Na_V1.4$ channels. Increasing $[Ca^{2+}]_i$ had no effect on the voltage dependence of activation (Fig. 7*A*) or steady-state inactivation (Fig. 7*B*) of $Na_v1.4$ channels expressed in HEK293 cells. The inactivation kinetics of $Na_V1.4$ currents expressed in either HEK293 cells (Fig. 7*C*) or $Na_V1.8$ null DRG neurons (data not shown) also were not altered by changes in $[Ca^{2+}]_i$. This indicates that the calcium-dependent calmodulin regulation of VGSC inactivation kinetics is isoform-specific.

Recently, Deschenes et al. (2002) reported that calcium/CaM shifted steady-state inactivation of $Na_v1.4$ currents in the negative direction by ~5 mV. Because we did not observe any shift in steady-state inactivation under our conditions, we performed additional sets of experiments that used conditions similar to those used by Deschenes and colleagues. The first set of experiments used the intracellular and bath solutions (Fig. 8) described by Deschenes et al. (2002) with no calcium buffering capacity in the pipette solution. No difference was observed in the voltage dependence of activation (Fig. 8*A*) or steady-state inactivation (Fig. 8*B*) between cells transfected with either $Na_v1.4$ plus CaM or $Na_v1.4$ plus EGFP. In the second set of experiments that used these solutions, the intracellular free calcium was buffered to ~10 μM with the addition of 1.1 mM EGTA and 1.1 mM $CaCl_2$ to the pipette solution. In this set of experiments we recorded from HEK293 cells that stably expressed $Na_v1.4$ channels with or without the addition of 10 μM CaM (Calbiochem) to the pipette solution. At 10 min after establishing the whole-cell recording configuration, we measured the voltage dependence of activation (Fig. 8*C*) and steady-state inactivation (Fig. 8*D*). Calcium/calmodulin did not alter the voltage dependence of $Na_v1.4$ currents under these conditions. Therefore, we conclude that calcium/calmodulin does not alter the voltage-dependent or kinetic properties of $Na_v1.4$ currents.

Discussion

In this study we describe the modulation of two VGSC isoforms, $Na_V1.4$ and $Na_V1.6$, by CaM and intracellular calcium. We show that functional expression of $Na_v1.4$ current is critically dependent on the ability of $Na_v1.4$ to bind CaM to its C terminus, indicating that this is a novel mechanism for the regulation of sodium current amplitude. Mutations in the IQ motif of $Na_V1.6$ channels also reduced $Na_V1.6$ current amplitude, although to a smaller extent than $Na_V1.4$ channels. We did not find any evidence that CaM modulated the voltage dependence of activation or inactivation of either $Na_v1.4$ or $Na_v1.6$ channels. However, we found that changes in the intracellular calcium ion concentration altered the inactivation kinetics of $Na_V1.6$ currents via a CaM-dependent mechanism. These data show that CaM can regulate the properties of VGSCs in isoform-specific ways and via both calcium-dependent and calcium-independent mechanisms.

The regulation of $Na_v1.4$ and $Na_v1.6$ current density by CaM was surprising, but not unprecedented. CaM appears to be an important regulator of several different ionic currents; recently, Saimi and Kung (2002) proposed that CaM could be considered a channel subunit in itself. The high voltage-activated sodium channels of *Paramecium* are critically dependent on CaM for activation (Saimi and Ling, 1995). CaM has been shown to interact with the C terminus of SK4 potassium channels, and this interaction controls channel assembly and surface expression of SK4 channels (Joiner et al., 2001). Functional expression of KCNQ2/Q3 potassium channels also requires CaM binding, al-

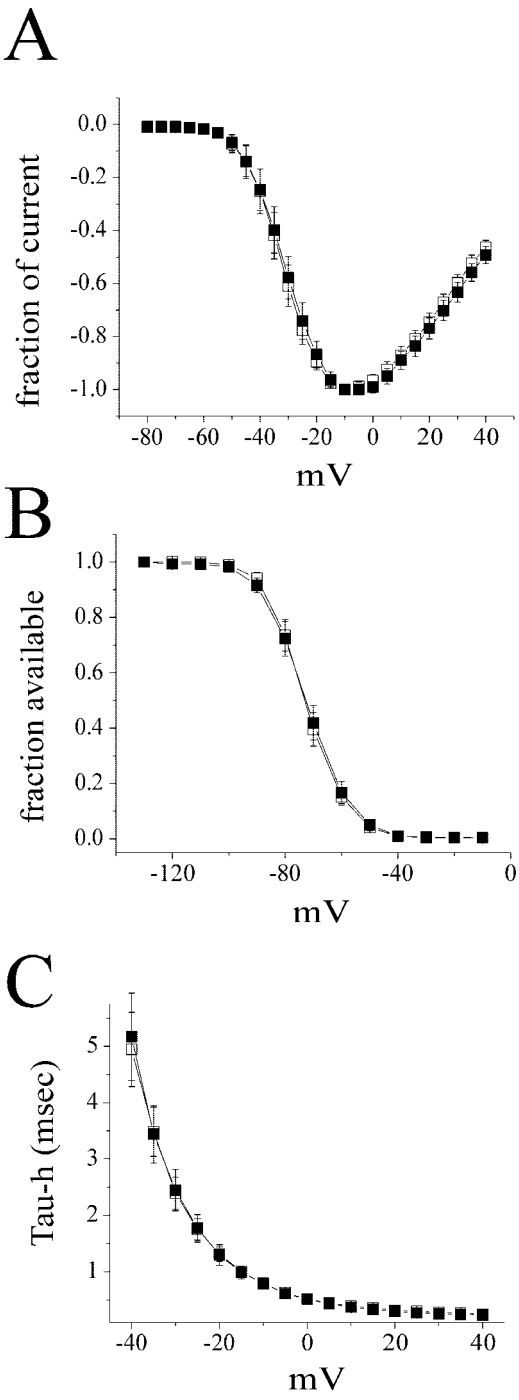

Figure 7. Calcium/CaM does not modulate $Na_v1.4$ inactivation kinetics or voltage-dependent properties. *A*, Normalized peak current–voltage relationship for $Na_v1.4$ channels recorded with low (filled squares; $n = 8$) and high (open squares; $n = 8$) intracellular calcium. The currents were elicited by 40 msec test pulses to various potentials from −80 to −40 mV. Cells were held at −120 mV. *B*, Comparison of $Na_v1.4$ steady-state inactivation recorded with low (filled squares; $n = 8$) and high (open squares; $n = 8$) intracellular calcium. Steady-state inactivation was estimated by measuring the peak current amplitude elicited by 20 msec test pulses to −10 mV after 500 msec prepulses to potentials over the range of −130 to −10 mV. Current is plotted as a fraction of the maximum peak current. *C*, Inactivation kinetics as a function of voltage for $Na_v1.4$ currents. The macroscopic decay time constant is similar for $Na_v1.4$ currents recorded with high intracellular calcium (open squares; $n = 8$) and with low intracellular calcium (filled squares; $n = 8$). Time constants were estimated from single exponential fits to the decay phase of currents elicited by 40 msec step depolarizations to the indicated potential. All recordings were made in the presence of 250 nM TTX from HEK293 cells transfected with TTX-resistant $Na_v1.4$ channels. Significant differences were determined using Student's *t* test with the significance value set at $p < 0.05$.

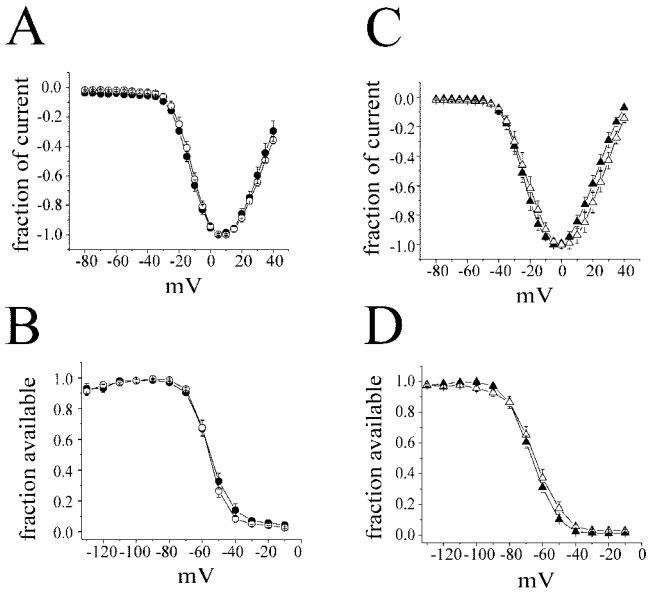

Figure 8. Calcium/CaM does not shift the voltage dependence of $Na_v1.4$ activation or steady-state inactivation. In these experiments the intracellular solution contained (in mM): 35 NaCl, 105 CsCl, and 10 Cs-HEPES, pH 7.3, and the extracellular solution contained (in mM): 150 NaCl, 2 KCl, 2 $CaCl_2$, 1 $MgCl_2$, 10 glucose, and 10 Na-HEPES, pH 7.4, as described by Deschenes et al. (2002). *A*, Normalized peak current–voltage relationship for $Na_v1.4$ channels recorded with no intracellular calcium buffering. HEK293 cells were cotransfected with $Na_v1.4$ channels and either EGFP (filled circles; $n = 5$) or CaM (open circles; $n = 5$). The currents were elicited by 40 msec test pulses to various potentials from −80 to −40 mV. Cells were held at −120 mV. *B*, Comparison of $Na_v1.4$ steady-state inactivation recorded with no intracellular calcium buffering. HEK293 cells were cotransfected with $Na_v1.4$ channels and either EGFP (filled circles; $n = 5$) or CaM–EGFP (open circles; $n = 5$). Steady-state inactivation was estimated by measuring the peak current amplitude elicited by 20 msec test pulses to −10 mV after 500 msec prepulses to potentials over the range of −130 to −10 mV. Current is plotted as a fraction of the maximum peak current. *C*, Normalized peak current–voltage relationship for $Na_v1.4$ channels recorded from HEK293 cells stably expressing $Na_v1.4$ channels with (open triangles; $n = 8$) or without (filled triangles; $n = 6$) 10 μM CaM in the pipette solution. The currents were activated as described in *A*. *D*, Comparison of $Na_v1.4$ steady-state inactivation recorded from HEK293 cells stably expressing $Na_v1.4$ channels with (open triangles; $n = 8$) or without (filled triangles; $n = 6$) 10 μM CaM in the pipette solution. The currents were elicited as described in *B*.

though in this case CaM is not required for targeting of KCNQ2 to the cell membrane despite the fact that KCNQ2 seems to bind CaM constitutively in a calcium-independent manner (Wen and Levitan, 2002).

Although CaM is expressed at relatively high concentrations (1–100 μM) in many cell types, CaM binding proteins may outnumber CaM by as much as 2:1. Persechini and Cronk (1999) estimated that, although under normal conditions high-affinity ($K_D \leq 10$ nM) CaM binding proteins are able to bind CaM, low-affinity ($K_D \geq 100$ nM) CaM binding proteins are able to bind CaM only if the local concentration of free CaM can be increased significantly. Mori et al. (2000) reported that affinity of the IQ motif of $Na_v1.2$ for CaM was 5 nM; therefore, $Na_v1.2$ would be considered a high-affinity CaM binding protein. Our data suggest that $Na_v1.4$ and $Na_v1.6$ also might be high-affinity CaM binding proteins (Fig. 1*B*) and might bind CaM constitutively. Indeed, although eliminating CaM binding to the IQ motif of $Na_v1.4$ or $Na_v1.6$ channels had major effects on current density, the overexpression of CaM did not seem to alter the properties of wild-type $Na_v1.4$ or $Na_v1.6$ currents, suggesting that the channels might be saturated with CaM. The fact that overexpression of CaM was able to increase the current amplitude in cells expressing $Na_v1.4$ or $Na_v1.6$ channels with IQ mutations that reduced, but that did not eliminate, current and CaM binding provides compelling evidence

for a direct regulation of sodium current amplitude by CaM. Interestingly, a recent study indicated that a mutation identified in the C terminus of the human $Na_v1.2$ channel (R1902C) from an individual with autism might reduce the binding affinity of $Na_v1.2$ for calcium/calmodulin (Weiss et al., 2003).

Our GST-fusion protein assays indicated that the C termini of $Na_v1.1$, $Na_v1.3$, and $Na_v1.7$ bound CaM with a lower affinity than the other TTX-sensitive isoforms. Although the IQ motifs of the various sodium channel isoforms are fairly well conserved, there are differences in this region (for example, $Na_v1.3$ has an asparagine at a position at which the other isoforms have an alanine; Fig. 1*A*), and these differences could alter CaM binding. However, it is likely that other regions in the C termini of the different isoforms also influence CaM binding. It will be interesting to determine whether CaM also can regulate the current density produced by the TTX-sensitive VGSC isoforms other than $Na_v1.4$ and $Na_v1.6$. None of the three known TTX-resistant isoforms ($Na_v1.5$, $Na_v1.8$, and $Na_v1.9$) showed detectable CaM binding in our assay. Two previous studies have suggested that $Na_v1.5$ might bind CaM. Tan et al. (2002) reported that a 20-amino-acid peptide containing the IQ motif of $Na_v1.5$ was able to bind CaM, and Deschenes et al. (2002) reported that a truncated form of the C terminus of $Na_v1.5$ that contained 53 amino acids was able to bind CaM. Our experiments were conducted by using the complete C terminus of $Na_v1.1$–$Na_v1.9$ for the *in vitro* binding studies, and, because regions outside the IQ motif can influence CaM binding (Peersen et al., 1997), conformational changes in the full-length C terminus might account for the lack of CaM binding to $Na_v1.5$ in our assay. Interestingly, Tan et al. (2002) reported that the 20 AA peptide containing the $Na_v1.5$ IQ motif showed a lower affinity for CaM than the 290–309 CaM antagonist peptide derived from CaM kinase II. Because the 290–309 peptide has an affinity for CaM of 52 nM (Payne et al., 1988), this indicates that the affinity of the $Na_v1.5$ IQ motif for CaM is >10-fold lower than that of the $Na_v1.2$ IQ motif. Based on these data, $Na_v1.5$ would be considered a low-affinity binding protein and would not be expected to bind CaM constitutively. Although the study by Tan et al. (2002) suggested that calcium/CaM might decrease the amplitude of $Na_v1.5$ currents by ~5–15% by regulating an intermediate form of slow inactivation, Deschenes et al. (2002) concluded that $Na_v1.5$ currents are modulated only indirectly by CaM via a CaM-dependent kinase.

We did not see any effect of CaM overexpression on the voltage-dependent properties of $Na_v1.4$ or $Na_v1.6$ currents. In contrast, Deschenes et al. (2002) reported that overexpression of CaM in HEK293 cells produced a −6 mV shift in the voltage dependence of steady-state inactivation of $Na_v1.4$ currents (Deschenes et al., 2002). Whereas we used 1.1 mM EGTA to buffer intracellular free calcium in our control experiments, Deschenes et al. (2002) did not include any calcium buffers in their intracellular solution for their control conditions. However, we also did not observe any effect of overexpression of CaM on $Na_v1.4$ currents when we used the solutions described by Deschenes and colleagues without intracellular calcium buffering. In unbuffered solutions the free calcium levels can be quite variable and even can be ≥10 μM (Pallotta et al., 1992). Therefore, we also examined the effect of adding CaM to the Deschenes et al. (2002) pipette solution when free calcium was buffered to ~10 μM with EGTA. Under these conditions the additional CaM had no effect on the voltage dependence of $Na_v1.4$ currents. We did not find any evidence that the properties of $Na_v1.4$ were regulated by CaM in a calcium-dependent manner in any of the experiments that we conducted.

Our data showed that the functional properties of $Na_v1.6$ currents are regulated by calcium/CaM, which slowed inactivation by ~50%. However, because the $Na_v1.6$-EE currents also exhibited slowed inactivation, our data indicate that calcium-free CaM enhances the rate of inactivation, and, when calcium binds to CaM, calcium/CaM disrupts this enhancement, thereby effectively slowing inactivation. By disrupting the binding of CaM to the IQ motif, the EE mutation effectively would prevent the calcium-free CaM enhancement of inactivation. Although in this proposed mechanism calcium-free CaM is the active molecule, which is the case for other actions of CaM (Jurado et al., 1999), this still represents a calcium-dependent modulation of sodium current properties. This is the first description of a calcium-dependent CaM modulation of a neuronal sodium channel isoform. CaM has been shown to confer calcium sensitivity to several other transmembrane channel proteins (Saimi and Kung, 1994; Levitan, 1999). The fact that we are now able to observe a similar regulatory mechanism for $Na_v1.6$, a neuronal VGSC that is present along axons (Caldwell et al., 2000) and extends to axon terminals (Black et al., 2002), has potentially interesting implications for the control of neuronal excitability and synaptic transmission by calcium/CaM. The calcium/CaM-dependent slowing of $Na_v1.6$ inactivation kinetics could prolong action potential duration, and in nerve terminals this type of modulation might enhance neurotransmitter release.

Conclusions

Our data show that CaM binding to the C terminus of VGSCs can be critical for obtaining functional sodium current expression and may provide a mechanism for regulating the amplitude of sodium currents in a concentration-dependent manner. Although our experiments with GST-fusion proteins indicate that CaM binding to the C terminus of VGSCs is not dependent on calcium concentration, calcium and CaM are known to play important roles in excitation contraction coupling in muscle (Hamilton et al., 2000) and in controlling the excitability of neurons (Sola et al., 2001), and the interaction of the CaM–VGSC complex with other proteins in neurons and muscle cells may be modulated by calcium. In addition, although we did not observe any calcium/CaM-dependent regulation of $Na_v1.4$ currents, the inactivation kinetics of $Na_v1.6$ currents were modulated by calcium/CaM. The array of mechanisms that involve finely tuned Ca^{2+} concentrations just below the cell membrane is growing, and our data add a new mechanism, mediated by CaM, to the ways in which VGSCs can be regulated.

References

Akopian AN, Souslova V, England S, Okuse K, Ogata N, Ure J, Smith A, Kerr BJ, McMahon SB, Boyce S, Hill R, Stanfa LC, Dickenson AH, Wood JN (1999) The tetrodotoxin-resistant sodium channel SNS has a specialized function in pain pathways. Nat Neurosci 2:541–548.

Bahler M, Rhoads A (2002) Calmodulin signaling via the IQ motif. FEBS Lett 513:107–113.

Black JA, Renganathan M, Waxman SG (2002) Sodium channel $Na_v1.6$ is expressed along nonmyelinated axons and it contributes to conduction. Mol Brain Res 105:19–28.

Burgess DL, Kohrman DC, Galt J, Plummer NW, Jones JM, Spear B, Meisler MH (1995) Mutation of a new sodium channel gene, Scn8a, in the mouse mutant "motor endplate disease." Nat Genet 10:461–465.

Burgoyne RD, Weiss JL (2001) The neuronal calcium sensor family of Ca^{2+}-binding proteins. Biochem J 353:1–12.

Caffrey JM, Eng DL, Black JA, Waxman SG, Kocsis JD (1992) Three types of sodium channels in adult rat dorsal root ganglion neurons. Brain Res 592:283–297.

Caldwell JH, Schaller KL, Lasher RS, Peles E, Levinson SR (2000) Sodium

channel $Na_v1.6$ is localized at nodes of Ranvier, dendrites, and synapses. Proc Natl Acad Sci USA 97:5616–5620.

Catterall WA (2000) From ionic currents to molecular mechanisms: the structure and function of voltage-gated sodium channels. Neuron 26:13–25.

Chin D, Means AR (2000) Calmodulin: a prototypical calcium sensor. Trends Cell Biol 10:322–328.

Cummins TR, Zhou J, Sigworth FJ, Ukomadu C, Stephan M, Ptacek LJ, Agnew WS (1993) Functional consequences of a sodium channel mutation causing hyperkalemic periodic paralysis. Neuron 10:667–678.

Cummins TR, Howe JR, Waxman SG (1998) Slow closed-state inactivation: a novel mechanism underlying ramp currents in cells expressing the hNE/PN1 sodium channel. J Neurosci 18:9607–9619.

Cummins TR, Dib-Hajj SD, Black JA, Akopian AN, Wood JN, Waxman SG (1999) A novel persistent tetrodotoxin-resistant sodium current in small primary sensory neurons. J Neurosci 19:RC43(1–6).

Cummins TR, Aglieco F, Renganathan M, Herzog R, Dib-Hajj SD, Waxman SG (2001) $Na_v1.3$ sodium channels: rapid repriming and slow closed-state inactivation display quantitative differences after expression in a mammalian cell line and in spinal sensory neurons. J Neurosci 21:5952–5961.

Deschenes I, Neyroud N, DiSilvestre D, Marban E, Yue DT, Tomaselli GF (2002) Isoform-specific modulation of voltage-gated Na^+ channels by calmodulin. Circ Res 90:E49–E57.

Dolmetsch RE, Pajvani U, Fife K, Spotts JM, Greenberg ME (2001) Signaling to the nucleus by an L-type calcium channel-calmodulin complex through the MAP kinase pathway. Science 294:333–339.

Erickson MG, Alseikhan BA, Peterson BZ, Yue DT (2001) Preassociation of calmodulin with voltage-gated Ca^{2+} channels revealed by FRET in single living cells. Neuron 31:973–985.

Goldin AL, Barchi RL, Caldwell JH, Hofmann F, Howe JR, Hunter JC, Kallen RG, Mandel G, Meisler MH, Netter YB, Noda M, Tamkun MM, Waxman SG, Wood JN, Catterall WA (2000) Nomenclature of voltage-gated sodium channels. Neuron 28:365–368.

Hamilton SL, Serysheva I, Strasburg GM (2000) Calmodulin and excitation–contraction coupling. News Physiol Sci 15:281–284.

Joiner WJ, Khanna R, Schlichter LC, Kaczmarek LK (2001) Calmodulin regulates assembly and trafficking of SK4/IK1 Ca^{2+}-activated K^+ channels. J Biol Chem 276:37980–37985.

Jurado LA, Chockalingam PS, Jarrett HW (1999) Apocalmodulin. Physiol Rev 79:661–682.

Klugbauer N, Lacinova L, Flockerzi V, Hofmann F (1995) Structure and functional expression of a new member of the tetrodotoxin-sensitive voltage-activated sodium channel family from human neuroendocrine cells. EMBO J 14:1084–1090.

Lee A, Wong ST, Gallagher D, Li B, Storm DR, Scheuer T, Catterall WA (1999) Ca^{2+}/calmodulin binds to and modulates P/Q-type calcium channels. Nature 399:155–159.

Levitan IB (1999) It is calmodulin after all! Mediator of the calcium modulation of multiple ion channels. Neuron 22:645–648.

Ling KY, Preston RR, Burns R, Kink JA, Saimi Y, Kung C (1992) Primary mutations in calmodulin prevent activation of the Ca^{2+}-dependent Na^+ channel in *Paramecium*. Proteins 12:365–371.

Liu CJ, Wang H, Lengyel P (1999) The interferon-inducible nucleolar p204 protein binds the ribosomal RNA-specific UBF1 transcription factor and inhibits ribosomal RNA transcription. EMBO J 18:2845–2854.

Marrion NV, Tavalin SJ (1998) Selective activation of Ca^{2+}-activated K^+ channels by co-localized Ca^{2+} channels in hippocampal neurons. Nature 395:900–905.

Mori M, Konno T, Ozawa T, Murata M, Imoto K, Nagayama K (2000) Novel interaction of the voltage-dependent sodium channel (VDSC) with calmodulin: does VDSC acquire calmodulin-mediated Ca^{2+} sensitivity? Biochemistry 39:1316–1323.

Pallotta BS, Blatz AL, Magleby KL (1992) Recording from calcium-activated potassium channels. Methods Enzymol 207:194–207.

Payne ME, Fong YL, Ono T, Colbran RJ, Kemp BE, Soderling TR, Means AR (1988) Calcium/calmodulin-dependent protein kinase II. Characterization of distinct calmodulin binding and inhibitory domains. J Biol Chem 263:7190–7195.

Peersen OB, Madsen TS, Falke JJ (1997) Intermolecular tuning of calmodulin by target peptides and proteins: differential effects on Ca^{2+} binding and implications for kinase activation. Protein Sci 6:794–807.

Persechini A, Cronk B (1999) The relationship between the free concentrations of Ca^{2+} and Ca^{2+}-calmodulin in intact cells. J Biol Chem 274:6827–6830.

Peterson BZ, DeMaria CD, Adelman JP, Yue DT (1999) Calmodulin is the Ca^{2+} sensor for Ca^{2+}-dependent inactivation of L-type calcium channels. Neuron 22:549–558.

Pitt GS, Zuhlke RD, Hudmon A, Schulman H, Reuter H, Tsien RW (2001) Molecular basis of calmodulin tethering and Ca^{2+}-dependent inactivation of L-type Ca^{2+} channels. J Biol Chem 276:30794–30802.

Putkey JA, Sweeney HL, Campbell ST (1989) Site-directed mutation of the trigger calcium-binding sites in cardiac troponin C. J Biol Chem 264:12370–12378.

Rhoads AR, Friedberg F (1997) Sequence motifs for calmodulin recognition. FASEB J 11:331–340.

Saimi Y, Kung C (1994) Ion channel regulation by calmodulin binding. FEBS Lett 350:155–158.

Saimi Y, Kung C (2002) Calmodulin as an ion channel subunit. Annu Rev Physiol 64:289–311.

Saimi Y, Ling KY (1995) *Paramecium* Na^+ channels activated by Ca^{2+}-calmodulin: calmodulin is the Ca^{2+} sensor in the channel gating mechanism. J Membr Biol 144:257–265.

Schaller KL, Krzemien DM, Yarowsky PJ, Krueger BK, Caldwell JH (1995) A novel, abundant sodium channel expressed in neurons and glia. J Neurosci 15:3231–3242.

Schultz J, Copley RR, Doerks T, Ponting CP, Bork P (2000) SMART: a web-based tool for the study of genetically mobile domains. Nucleic Acids Res 28:231–234.

Smith MR, Smith RD, Plummer NW, Meisler MH, Goldin AL (1998) Functional analysis of the mouse Scn8a sodium channel. J Neurosci 18:6093–6102.

Sola C, Barron S, Tusell JM, Serratosa J (2001) The Ca^{2+}/calmodulin system in neuronal hyperexcitability. Int J Biochem Cell Biol 33:439–455.

Tan HL, Kupershmidt S, Zhang R, Stepanovic S, Roden DM, Wilde AA, Anderson ME, Balser JR (2002) A calcium sensor in the sodium channel modulates cardiac excitability. Nature 415:442–447.

Trimmer JS, Cooperman SS, Tomiko SA, Zhou JY, Crean SM, Boyle MB, Kallen RG, Sheng ZH, Barchi RL, Sigworth FJ (1989) Primary structure and functional expression of a mammalian skeletal muscle sodium channel. Neuron 3:33–49.

Tzoumaka E, Tischler AC, Sangameswaran L, Eglen RM, Hunter JC, Novakovic SD (2000) Differential distribution of the tetrodotoxin-sensitive rPN4/NaCh6/Scn8a sodium channel in the nervous system. J Neurosci Res 60:37–44.

Ukomadu C, Zhou J, Sigworth FJ, Agnew WS (1992) μI Na^+ channels expressed transiently in human embryonic kidney cells: biochemical and biophysical properties. Neuron 8:663–676.

Voit R, Schafer K, Grummt I (1997) Mechanism of repression of RNA polymerase I transcription by the retinoblastoma protein. Mol Cell Biol 17:4230–4237.

Weiss LA, Escayg A, Kearney JA, Trudeau M, MacDonald BT, Mori M, Reichert J, Buxbaum JD, Meisler MH (2003) Sodium channels SCN1A, SCN2A, and SCN3A in familial autism. Mol Psychiatry 8:186–194.

Weiss RE, Horn R (1986) Functional differences between two classes of sodium channels in developing rat skeletal muscle. Science 233:361–364.

Wellmann H, Kaltschmidt B, Kaltschmidt C (1999) Optimized protocol for biolistic transfection of brain slices and dissociated cultured neurons with a hand-held gene gun. J Neurosci Methods 92:55–64.

Wen H, Levitan IB (2002) Calmodulin is an auxiliary subunit of KCNQ2/3 potassium channels. J Neurosci 22:7991–8001.

Zhu H, Bilgin M, Bangham R, Hall D, Casamayor A, Bertone P, Lan N, Jansen R, Bidlingmaier S, Houfek T, Mitchell T, Miller P, Dean RA, Gerstein M, Snyder M (2001) Global analysis of protein activities using proteome chips. Science 293:2101–2105.

Zuhlke RD, Pitt GS, Deisseroth K, Tsien RW, Reuter H (1999) Calmodulin supports both inactivation and facilitation of L-type calcium channels. Nature 399:159–162.

Zuhlke RD, Pitt GS, Tsien RW, Reuter H (2000) Ca^{2+}-sensitive inactivation and facilitation of L-type $Ca2^+$ channels both depend on specific amino acid residues in a consensus calmodulin-binding motif in the α_{1C} subunit. J Biol Chem 275:21121–21129.